

# Enhancement of trapped field and total trapped flux on GdBaCuO bulk by the MMPSC + IMRA method

Hiroyuki Fujishiro<sup>1</sup>, Takuya Hiyama<sup>1</sup>, Tomoyuki Naito<sup>1</sup>,  
Yousuke Yanagi<sup>2</sup> and Yoshitaka Itoh<sup>2</sup>

<sup>1</sup> Faculty of Engineering, Iwate University, 4-3-5 Ueda, Morioka 020-8551, Japan

<sup>2</sup> IMRA Material R&D Company Limited, 2-1 Asahi-cho, Kariya 448-0032, Japan

E-mail: [fujishiro@iwate-u.ac.jp](mailto:fujishiro@iwate-u.ac.jp)

Received 25 March 2009, in final form 2 June 2009

Published 5 August 2009

Online at [stacks.iop.org/SUST/22/095006](http://stacks.iop.org/SUST/22/095006)

## Abstract

The trapped field  $B_T^P(z)$  and the total trapped flux  $\Phi_T(z)$  as a function of the distance  $z$  from the bulk surface have been measured on a GdBaCuO superconducting bulk of 45 mm in diameter, which was magnetized by a sequential pulsed field application (SPA) method, a modified multi-pulse technique with stepwise cooling (MMPSC), and a subsequent iterative magnetizing operation with gradually reduced pulse field amplitude (IMRA). A trapped field of  $B_T^P = 3.10$  T was realized by the MMPSC method, which was higher than that attained by SPA ( $B_T^P = 2.35$  T).  $\Phi_T(0.5$  mm), which was 1.64 mWb after the MMPSC method, was enhanced by about 53%, to 2.51 mWb, by the subsequent IMRA method due to the additional flux trapping. The MMPSC method combined with the IMRA process (MMPSC + IMRA) is an effective and promising pulse field magnetizing technique to enhance both  $B_T^P$  and  $\Phi_T$  on any superconducting bulks.

## 1. Introduction

Recently, practical applications using REBaCuO superconducting bulks (RE: rare earth ions and Y) as a strong quasi-permanent magnet have been intensively investigated for magnetic separation for environmental cleaning [1], a drug delivery system (DDS) for medical applications [2] and a sputtering cathode to grow thin films for semiconductor devices [3]. For the magnetic separation and the DDS, it is necessary to enhance not only the magnetic field  $B$ , but also the magnetic field gradient ( $\text{grad } B$ ) in order to achieve a stronger magnetic force. On the other hand, for the sputtering cathode and the motor/generator applications [4], a large amount of total trapped flux  $\Phi_T$  with a flat magnetic field distribution is necessary to make the uniform magnetic field reach farther away.

In the applications, the magnetizing technique of the superconducting bulks is very important. A field-cooled magnetization (FCM) is the conventional method and the trapped field  $B_T^{\text{FC}}$  and the total trapped flux  $\Phi_T^{\text{FC}}$  by FCM are as high as the maximum abilities of the bulk. Recently, a pulsed field magnetization (PFM) has been intensively studied

because of its compact, mobile and inexpensive setup. The trapped field  $B_T^P$  by PFM was, however, pretty small compared with  $B_T^{\text{FC}}$ , due to the large temperature rise from the dynamical motion of the magnetic flux. The maximum  $B_T^P$  ever reported is as low as 3.8 T at 30 K from an iteratively magnetizing pulsed field method with reducing amplitude (IMRA) [5]. We have systematically studied the time and spatial dependences of the temperature  $T(t, x)$ , local field  $B_L(t)$  and trapped field  $B_T^P$  on the surface of cryocooled REBaCuO bulks during PFM for various starting temperatures  $T_s$  and applied fields  $B_{\text{ex}}$ , and have suggested the importance of the precise measurements of  $T(t, x)$  on the bulk surface [6, 7].

To enhance  $B_T^P$ , the reduction in temperature rise  $\Delta T$  is an indispensable issue. The lowering of  $T_s$  down to 10–20 K, which is effective for FCM due to the enhancement of the critical current density  $J_c$ , is not necessarily effective for PFM because of the large heat generation due to the increase of pinning loss and the decrease of the specific heat of the bulk material. Taking the obtained experimental results into consideration, we proposed a new PFM technique named a modified multi-pulse technique with stepwise cooling (MMPSC) [8], and have attained the highest field trapping of

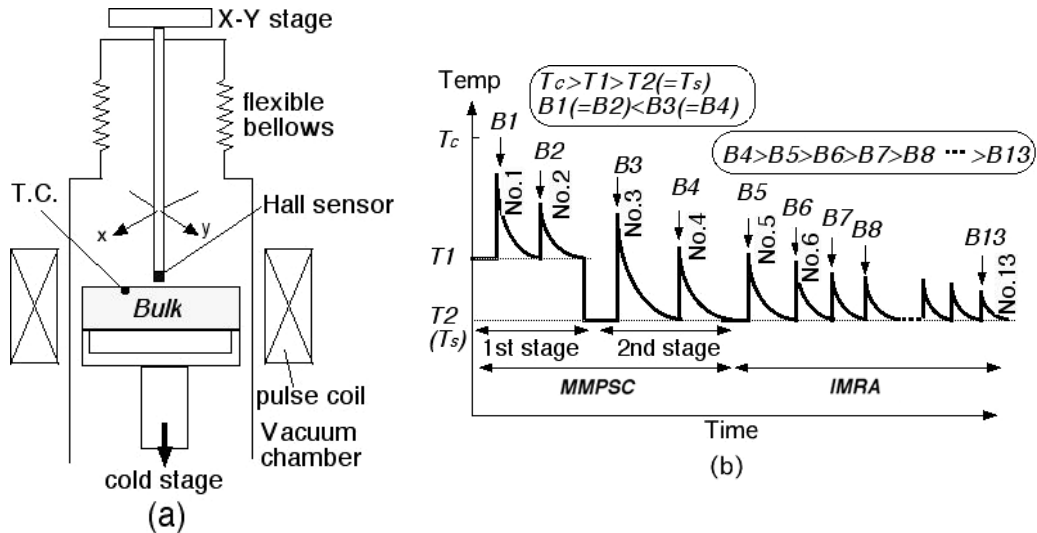


**Figure 1.** (a) The experimental setup around the bulk and the magnetizing pulse coil. (b) The experimental sequence of the MMPSC + IMRA technique.

$B_T^P = 5.20$  T at 29 K on a GdBaCuO bulk of 45 mm in diameter, on which only 3.6 T was trapped by a single pulse application at 40 K [9].  $B_T^P = 5.20$  T is the highest recorded value by PFM to date. We applied the technique to other bulks with different pinning ability and confirmed that the MMPSC was a universal and effective method to enhance  $B_T^P$  [10].

The IMRA method has been reported to be valuable for the enhancement of the  $\Phi_T$  value [5]. The MMPSC method followed by the IMRA method is expected to enhance both  $B_T^P$  and  $\Phi_T$  values. In the previous paper, we reported  $B_T^P$  (5 mm) and  $\Phi_T$  (5 mm) on a SmBaCuO bulk using the MMPSC + IMRA method, on which the  $\Phi_T$  (5 mm) value was enhanced by the subsequent IMRA method [11]. However, the  $B_T^P(z)$  and  $\Phi_T(z)$  values as a function of the distance  $z$  from the bulk surface have not been systematically investigated.

In this paper, we applied the PFM techniques to the GdBaCuO bulk with a higher trapped field ( $B_T^{FC} = 1.8$  T at 77 K) than that on the SmBaCuO bulk. The trapped field  $B_T^P(z)$  and the total trapped flux  $\Phi_T(z)$  are investigated as a function of the distance  $z$  for the MMPSC and the subsequent IMRA methods.

## 2. Experimental details

A GdBaCuO bulk superconductor (Nippon steel) with a 45 mm diameter and 15 mm thickness was used in this study. The trapped field  $B_T^{FC}$  and the total trapped flux  $\Phi_T^{FC}$  by FCM were as high as 1.80 T and 0.84 mWb, respectively, at 77 K on the bulk surface. A stainless-steel (SUS304) ring with a 6.0 mm thickness and 15 mm height was fixed onto the bulk disk using epoxy resin (Stycast 2850GT) to enhance the mechanical strength of the bulk and to reduce the temperature rise due to the increase in heat capacity [12].

Figure 1(a) shows the experimental setup around the bulk and the magnetizing pulse coil. The bulk was mounted on a soft iron yoke cylinder of 40 mm in diameter and 20 mm in

thickness and tightly anchored onto the cold stage of a Gifford–McMahon (GM) cycle helium refrigerator. The temperature of the bulk  $T_s$  was controlled over the range from 30 to 70 K. The bulk was magnetized using a copper pulse coil ( $L = 1.08$  mH and  $R = 0.25 \Omega$  at 100 K) dipped in liquid  $N_2$ , which was placed outside the vacuum chamber. The applied field  $\mu_0 H_a(t)$ , of which the maximum strength was defined as  $B_{ex}$ , was monitored by observing the current  $I(t)$  flowing through the shunt resistor. The maximum  $B_{ex}$  was 6.3 T and the rise time of the pulsed field was 12 ms. Three magnetic pulses with the same amplitude  $B_{ex}$ , which were named the 1st, 2nd and 3rd pulse, were applied to the bulk sequentially after re-cooling to  $T_s$ . We abbreviate this technique as the sequential pulsed field application (SPA) method. The trapped field characteristics of the bulk for the 1st pulse were reported elsewhere [13]. The trapped field profile  $B_T$  (0.5 mm) was measured 0.5 mm above the bulk surface by scanning an axial-type Hall sensor (F W Bell, BHA921) inside the vacuum chamber using a scanning device, which has an  $x$ – $y$  stage controller with flexible bellows. The total amount of the trapped magnetic flux density  $\Phi_T = \Phi_T$  (0.5 mm) was calculated by integrating the  $B_T$  (0.5 mm) value over the region where it was positive. The  $B_T^P(z)$  at the bulk center and the  $\Phi_T(z)$  values were also measured as a function of the distance  $z$ .

Figure 1(b) shows the experimental sequence of the MMPSC + IMRA technique. In the MMPSC part, four magnetic pulses were applied at different initial temperatures  $T_1$  and  $T_2$  on the bulk surface. At the first stage, a pulse field of  $B_1 (=B_2 = 3.3$  T) was applied twice at  $T_1 = 70$  K in order to realize the concave-shaped profile of the trapped field on the bulk. Hereafter, we refer to these two pulses as No. 1 and No. 2. At the second stage, the bulk was cooled down to  $T_2 = 30$  K and a higher pulse field  $B_3 (=B_4 = 6.3$  T) was applied twice (No. 3 and No. 4), after recovering to  $T_2$ . After the termination of the MMPSC part with pulse No. 4, the IMRA process is started to enhance the  $\Phi_T$  value, in which

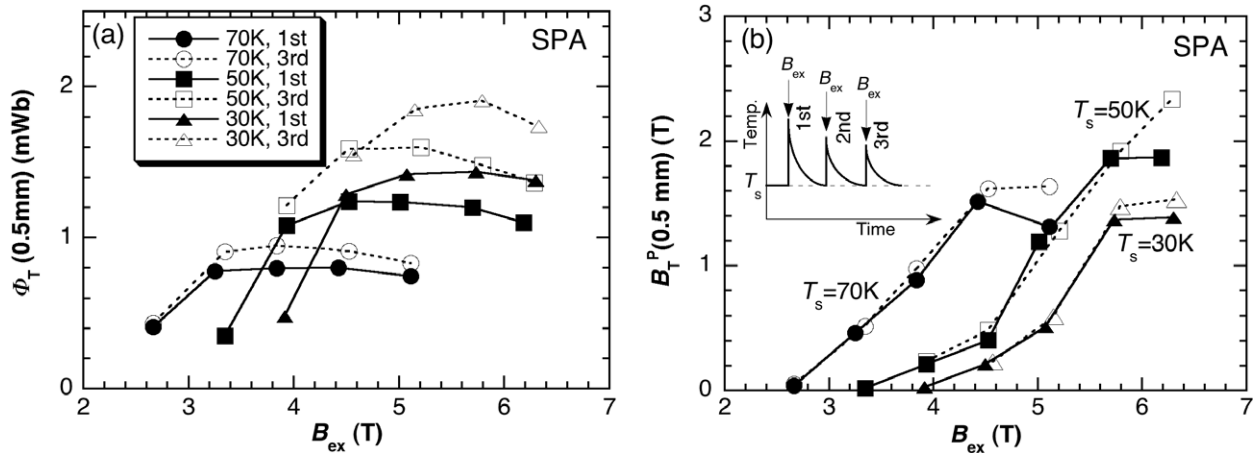


**Figure 2.** (a) The total trapped flux  $\Phi_T$  (0.5 mm) and (b) the trapped field  $B_T^P = B_T$  (0.5 mm) at the bulk center, after the 1st and 3rd pulses in the SPA process, as a function of the applied field  $B_{ex}$  for various temperatures  $T_s$ . In the inset of (b), the concept of the SPA process is schematically shown.

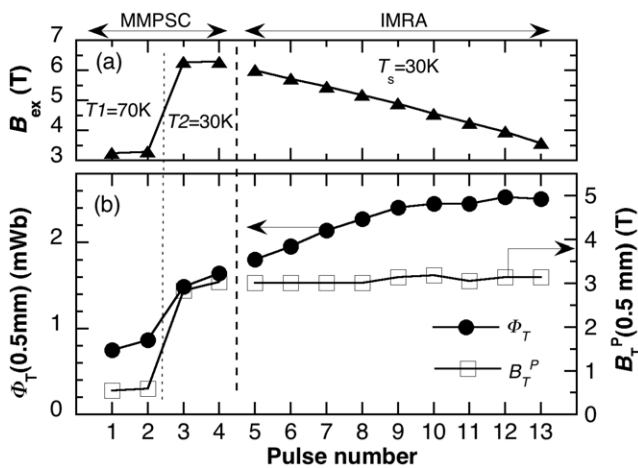


**Figure 3.** The pulse number dependence of (a) the applied field  $B_{ex}$  and (b) the total trapped flux  $\Phi_T$  (the left ordinates) and the trapped field  $B_T^P$  (right ordinates) for the MMPSC + IMRA method.

several magnetizing pulsed fields with reduced amplitude were iteratively applied to the bulk at  $T_s = 30$  K.

### 3. Results and discussion

#### 3.1. Sequential pulsed field application (SPA)

In order to investigate the field trapping ability of the GdBaCuO bulk used, it was magnetized by a single pulse application and SPA, both of which are conventional techniques in PFM. Figure 2(a) shows the total trapped flux  $\Phi_T = \Phi_T$  (0.5 mm) after the 1st and 3rd pulse application in SPA as a function of the applied field  $B_{ex}$  at  $T_s = 70$ , 50 and 30 K. All the  $\Phi_T$ - $B_{ex}$  curves take a maximum. The maximum  $\Phi_T$  value increases, and the  $B_{ex}$  value, at which  $\Phi_T$  takes a maximum, shifts to a higher value with decreasing  $T_s$ . It should be noted that the  $\Phi_T$  value increases noticeably for the SPA technique; the  $\Phi_T$  value for the 3rd pulse was 20–40% larger than that for the 1st pulse at each  $T_s$ , and also that the

increment rate increased with decreasing  $T_s$ . In this way, the SPA technique is effective for the enhancement of  $\Phi_T$ .

Figure 2(b) shows the trapped field  $B_T^P = B_T$  (0.5 mm) at the bulk center after the 1st and 3rd magnetic pulse application, as a function of  $B_{ex}$  at various  $T_s$ . For the 1st pulse,  $B_T^P$  at  $T_s = 70$  K starts to increase for  $B_{ex} \geq 2.7$  T, takes a maximum at  $B_{ex} = 4.5$  T and then decreases with increasing  $B_{ex}$ . The  $B_T^P$ - $B_{ex}$  curve can usually be observed for PFM techniques, which is attributed to a large temperature rise in the bulk for higher  $B_{ex}$ , due to the fast motion of the magnetic flux lines in the presence of resistive forces; the pinning force  $F_p$  and the viscous force  $F_v$ . The applied pulsed field, at which the magnetic flux starts to be trapped at the bulk center, increases with decreasing  $T_s$ , which comes from the increase of the shielding current in the superconductor. For the 1st pulse application, the maximum  $B_T^P$  was 1.90 T at 50 K for  $B_{ex} = 6.3$  T and was enhanced to 2.35 T for the 3rd pulse application in SPA. The slight increase in the  $B_T^P$  value for the 3rd pulse comes from the decrease of the temperature rise [10].

#### 3.2. MMPSC + IMRA method

In a previous paper, we investigated the optimization of the MMPSC method for the bulk used in this study [13]. As a result, the conditions ( $T1 = 70$  K,  $B1 = B2 = 3.3$  T,  $T2 = 30$  K,  $B3 = B4 = 6.3$  T) were confirmed to be the optimum ones to attain a higher  $B_T^P$  than 3 T on the bulk surface. Figure 3(a) shows the pulse number dependence of the applied field  $B_{ex}$  for the MMPSC + IMRA method. In the IMRA part, the applied field  $B_{ex}$  was decreased step by step from 6.01 T (No. 5 pulse) to 3.58 T (No. 13 pulse) at  $T_s = 30$  K. Figure 3(b) shows the pulse number dependence of the total trapped flux  $\Phi_T = \Phi_T$  (0.5 mm) and the trapped field  $B_T^P = B_T$  (0.5 mm) for the MMPSC + IMRA method.  $B_T^P$  was drastically enhanced to 2.95 T for the No. 3 pulse and 3.10 T for the No. 4 pulse in the MMPSC part, due to the cone-shaped field trapping and, as a result,  $\Phi_T$  was also enhanced to 1.64 mWb for the No. 4 pulse. In the IMRA part,  $\Phi_T$  gradually increases and tends to saturate for  $n \geq 10$ ;

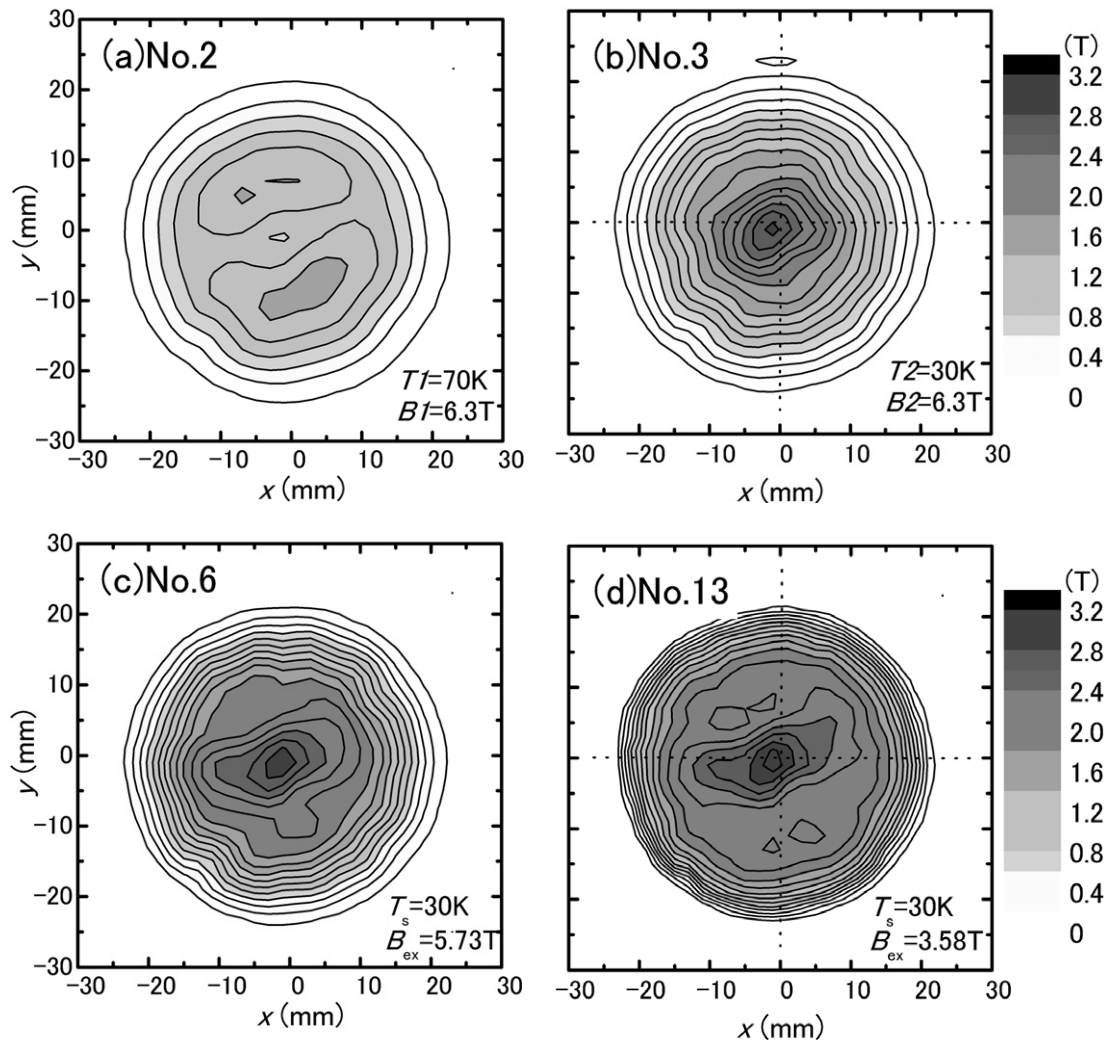


**Figure 4.** The trapped field  $B_T = B_T(0.5 \text{ mm})$  profiles for the (a) No. 2 and (b) No. 3 pulses in the MMPSC part, and (c) No. 6 and (d) No. 13 pulses in the IMRA part in the MMPSC + IMRA method.

**Table 1.** Summary of the  $\Phi_T(z)$  and  $B_T^P(z)$  values. The decrement rates  $\Phi_T(z)/\Phi_T(0.5 \text{ mm})$  and  $B_T^P(z)/B_T^P(0.5 \text{ mm})$  are also shown in parentheses.

Method	$z = 0.5 \text{ mm}$	$z = 5 \text{ mm}$	$z = 10 \text{ mm}$	$z = 20 \text{ mm}$
MMPSC	$\Phi_T = 1.64 \text{ mWb}$	$\Phi_T = 1.17 \text{ mWb}$ (71%)	$\Phi_T = 0.86 \text{ mWb}$ (52%)	$\Phi_T = 0.49 \text{ mWb}$ (29%)
	$B_T^P = 3.10 \text{ T}$	$B_T^P = 1.63 \text{ T}$ (53%)	$B_T^P = 0.99 \text{ T}$ (32%)	$B_T^P = 0.42 \text{ T}$ (14%)
MMPSC + IMRA	$\Phi_T = 2.51 \text{ mWb}$	$\Phi_T = 1.79 \text{ mWb}$ (71%)	$\Phi_T = 1.30 \text{ mWb}$ (52%)	$\Phi_T = 0.72 \text{ mWb}$ (29%)
	$B_T^P = 3.14 \text{ T}$	$B_T^P = 1.86 \text{ T}$ (59%)	$B_T^P = 1.21 \text{ T}$ (39%)	$B_T^P = 0.56 \text{ T}$ (18%)

$\Phi_T = 2.44 \text{ mWb}$  (No. 10) and  $\Phi_T = 2.51 \text{ mWb}$  (No. 13). The  $\Phi_T$  behavior in the IMRA part comes from the additional flux trapping due to the smaller temperature rise, which results from the lower  $B_{ex}$ . The IMRA process might be ineffective for a lower  $B_{ex}$  than the critical value, even if the pulse number increases. On the other hand,  $B_T^P$  is slightly increased from 3.10 T (No. 4) to 3.14 T (No. 13) during the IMRA process, which suggests that additional magnetic flux might be trapped at the bulk periphery.

Figure 4 shows the  $B_T(0.5 \text{ mm})$  profiles for a typical step in the MMPSC + IMRA method. In figure 4(a) for the No. 2 pulse in the MMPSC part, the magnetic flux is trapped with a concave distribution due to the lower  $B_{ex}$ , which can be understood on the basis of Bean's critical state model. For the No. 3 pulse application, the  $B_T$  profile changes to a convex one as shown in figure 4(b), which indicates that a large amount of magnetic flux intrudes into the bulk center. In figure 4(c) for the No. 6 pulse in the IMRA part, most of the magnetic flux

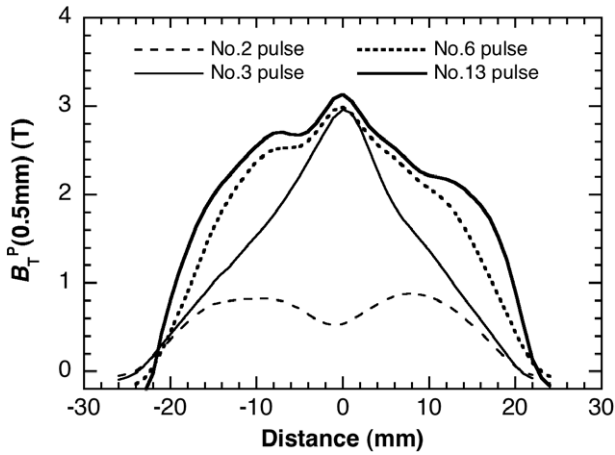


**Figure 5.** The cross section of the  $B_T(0.5\text{ mm})$  profiles for each step of the MMPSC + IMRA method.

is trapped at the bulk periphery, and finally for the No. 13 pulse, the magnetic flux is additionally trapped as shown in figure 4(d).

Figure 5 shows the cross sections of the  $B_T(0.5\text{ mm})$  profiles along the  $x$ -axis shown in figure 4 for each step in the MMPSC + IMRA method. For the No. 2 pulse, a small amount of magnetic flux was trapped on the bulk periphery and a concave or ‘M-shaped’ profile was observed. After the No. 3 pulse application, a cone-shaped profile with a higher  $B_T^C$  can be observed. As shown in figures 4(c) and (d), the magnetic flux is trapped at the bulk periphery.

### 3.3. The distance $z$ dependence of $\Phi_T(z)$ and $B_T^C(z)$

We measured the total trapped flux  $\Phi_T(z)$  and the trapped field  $B_T^P(z)$  as a function of the distance  $z$ . Table 1 summarizes the  $\Phi_T(z)$  and  $B_T^P(z)$  values after the MMPSC part (No. 4) and the IMRA part (No. 13), in which the decrement rate of  $\Phi_T(z)$  and  $B_T^P(z)$  compared with those at  $z = 0.5\text{ mm}$  are also shown in parentheses. Figure 6(a) shows the results of  $\Phi_T(z)$ . By performing the IMRA process, the  $\Phi_T(0.5\text{ mm})$  value after

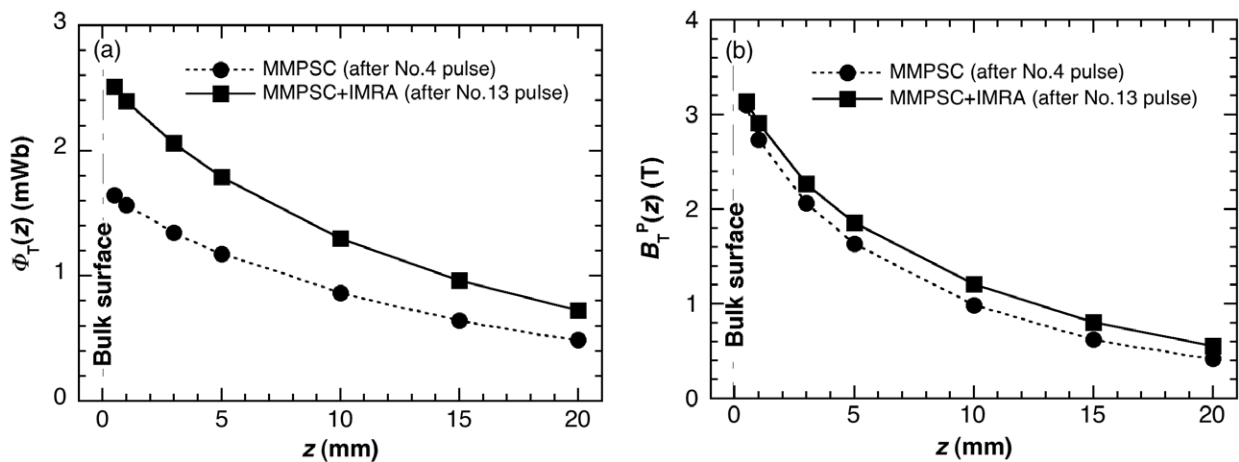
the No. 13 pulse was enhanced to 2.51 mWb, which was 53% larger than that after the No. 4 pulse (1.64 mWb).  $\Phi_T(z)$  for the No. 4 and No. 13 pulse decreases with increasing  $z$  and the decrement rate is nearly the same;  $\Phi_T(z)/\Phi_T(0.5\text{ mm})$  for  $z = 10$  and 20 mm is 52% and 29%, respectively.

Figure 6(b) shows the results of  $B_T^P(z)$ . Similarly to the results of  $\Phi_T(z)$ ,  $B_T^P(z)$  monotonously decreases with increasing  $z$ . The decrement rate of  $B_T^P(z)$  in the MMPSC + IMRA method is slightly smaller than that in the MMPSC method;  $B_T^C(z)(20\text{ mm})/B_T(0.5\text{ mm})$  for the MMPSC and MMPSC + IMRA is 14% and 18%, respectively.

## 4. Summary

The trapped field  $B_T^P$  and the total trapped flux  $\Phi_T(z)$  as a function of the distance  $z$  from the bulk surface have been investigated on a GdBaCuO superconducting bulk which was magnetized by a sequential pulsed field application (SPA) method, a modified multi-pulse technique with stepwise cooling (MMPSC), and a subsequent iterative magnetizing operation with gradually reduced pulse field amplitude (IMRA). The important experimental results and conclusions obtained in this study are summarized as follows.

- (1) A trapped field of  $B_T^P = 3.10\text{ T}$  was realized at  $T_2 = 30\text{ K}$  at the end of the MMPSC method (No. 4 pulse), which was higher than that attained by SPA at 50 K ( $B_T^P = 2.35\text{ T}$  for the 3rd pulse). The  $B_T^P$  of 3.10 T was slightly enhanced to 3.14 T by the subsequent IMRA method. The MMPSC method is valuable to enhance the trapped field at the bulk center.
- (2)  $\Phi_T(0.5\text{ mm})$  after the MMPSC method was 1.64 mWb, which was enhanced significantly to 2.51 mWb by the subsequent IMRA method due to additional flux trapping.
- (3) The MMPSC method combined with the IMRA process (MMPSC + IMRA) is an effective and promising pulse field magnetization technique for enhancing both  $B_T^P$  and  $\Phi_T$  on any superconducting bulks.



**Figure 6.** (a) The total trapped flux  $\Phi_T(z)$  and (b) the trapped field  $B_T^P(z)$  as a function of the distance  $z$  from the bulk surface for the MMPSC + IMRA method. The results after the No. 4 and No. 13 pulse application, respectively, are indicated.

## Acknowledgments

This work is supported in part by a Grant-in-Aid for Scientific Research from the Ministry of Education, Culture, Sports, Science and Technology, Japan (No. 19560003).

## References

- [1] Hayashi H, Tsutsumi K, Saho N, Nishizima N and Asano K 2003 *Physica C* **392–396** 745
- [2] Mishima F, Takeda S, Izumi Y and Nishijima S 2006 *IEEE Trans. Appl. Supercond.* **17** 2303
- [3] Yanagi Y, Matsuda T, Hazama H, Yokouchi K, Yoshikawa M, Itoh Y, Oka T, Ikuta H and Mizutani U 2005 *Physica C* **426–431** 764
- [4] Miki M *et al* 2006 *Supercond. Sci. Technol.* **19** S494
- [5] Yanagi Y, Itoh Y, Yoshikawa M, Oka T, Hosokawa T, Ishihara H and Ikuta H and Mizutani U 2000 *Advances in Superconductivity XII* (Tokyo: Springer) p 470
- [6] Fujishiro H, Oka T, Yokoyama K, Kaneyama M and Noto K 2004 *IEEE Trans. Appl. Supercond.* **14** 1054
- [7] Fujishiro H, Yokoyama K, Oka T and Noto K 2004 *Supercond. Sci. Technol.* **17** 51
- [8] Fujishiro H, Kaneyama M, Tateiwa T and Oka T 2005 *Japan. J. Appl. Phys.* **44** L1221
- [9] Fujishiro H, Tateiwa T, Fujiwara A, Oka T and Hayashi H 2006 *Physica C* **445–448** 334
- [10] Fujishiro H, Tateiwa T, Kakehata K, Hiyama T, Naito T and Yanagi Y 2008 *Physica C* **468** 1477
- [11] Fujishiro H, Tateiwa T and Hiyama T 2007 *Japan. J. Appl. Phys.* **46** 4108
- [12] Fujishiro H, Yokoyama K, Kaneyama M, Oka T and Noto K 2005 *IEEE Trans. Appl. Supercond.* **15** 3762
- [13] Fujishiro H, Hiyama T, Tateiwa T, Yanagi Y and Oka T 2007 *Physica C* **463–465** 394